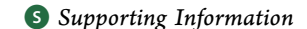


pubs.acs.org/est

Global Sources of Fine Particulate Matter: Interpretation of PM_{2.5} Chemical Composition Observed by SPARTAN using a Global Chemical Transport Model

Crystal L. Weagle,*,a,b,o Graydon Snider,b Chi Li,b,o Aaron van Donkelaar,b Sajeev Philip,b,c Paul Bissonnette,b Jaqueline Burke,b John Jackson,b Robyn Latimer,b Emily Stone,b Ihab Abboud,d Clement Akoshile,b Nguyen Xuan Anh,o Jeffrey Robert Brook,f Aaron Cohen,g Jinlu Dong,h Mark D. Gibson,b Derek Griffith, Kebin B. He,b Brent N. Holben,k Ralph Kahn,k Christoph A. Keller,l,m Jong Sung Kim, Nofel Lagrosas,o Puji Lestari,p Yeo Lik Khian,q Yang Liu,ro Eloise A. Marais,so J. Vanderlei Martins,b Amit Misra,u Ulfi Muliane,p Rizki Pratiwi,p Eduardo J. Quel,v Abdus Salam,w Lior Segev,x Sachchida N. Tripathi,u Chien Wang,q Qiang Zhang,b Michael Brauer,y Yinon Rudich,xo and Randall V. Martinab,z

^zHarvard-Smithsonian Center for Astrophysics, Cambridge, Massachusetts 02138, United States



Received: March 28, 2018
Revised: September 12, 2018
Accepted: September 14, 2018
Published: September 14, 2018



^aDepartment of Chemistry, Dalhousie University, Halifax, Nova Scotia B3H 4R2, Canada

^bDepartment of Physics and Atmospheric Science, Dalhousie University, Halifax, Nova Scotia B3H 4R2, Canada

^cNASA Ames Research Center, Moffett Field, California 94035-0001, United States

dCentre for Atmospheric Research Experiments, Environment and Climate Change Canada, Egbert, Ontario L0L 1N0, Canada

¹Department of Physics, University of Ilorin, Ilorin, Nigeria

^eInstitute of Geophysics, Vietnam Academy of Science and Technology, Hanoi, Vietnam

Department of Public Health Sciences, University of Toronto, Toronto, Ontario MSS 1A8, Canada

^gHealth Effects Institute, Boston, Massachusetts 02110-1817, United States

^hDepartment of Earth System Science, Tsinghua University, Beijing 100084, China

ⁱDepartment of Civil and Resource Engineering, Dalhousie University, Halifax, Nova Scotia B3H 4R2, Canada

^jCouncil for Scientific and Industrial Research (CSIR), Pretoria, South Africa 0001

^kEarth Science Division, NASA Goddard Space Flight Center, Greenbelt, Maryland 21046, United States

¹Universities Space Research Association/Goddard Earth Science Technology and Research, Columbia, Maryland 20771, United States

^mGlobal Modeling and Assimilation Office, NASA Goddard Space Flight Center, Greenbelt, Maryland 20771, United States

ⁿDepartment of Community Health and Epidemiology, Dalhousie University, Halifax, Nova Scotia B3H 4R2, Canada

^oManila Observatory, Ateneo de Manila University campus, Quezon City, 1108, Philippines

PFaculty of Civil and Environmental Engineering, ITB, JL. Ganesha No.10, Bandung 40132, Indonesia

^qCenter for Global Change Science, Massachusetts Institute of Technology, Cambridge, Massachusetts 02139, United States

^rRollins School of Public Health, Emory University, Atlanta, Georgia 30322, United States

^sSchool of Geography, Earth and Environmental Sciences, University of Birmingham, Birmingham B15 2TT, United Kingdom ^tDepartment of Physics and Joint Center for Earth Systems Technology, University of Maryland, Baltimore County, Baltimore, Maryland 21201, United States

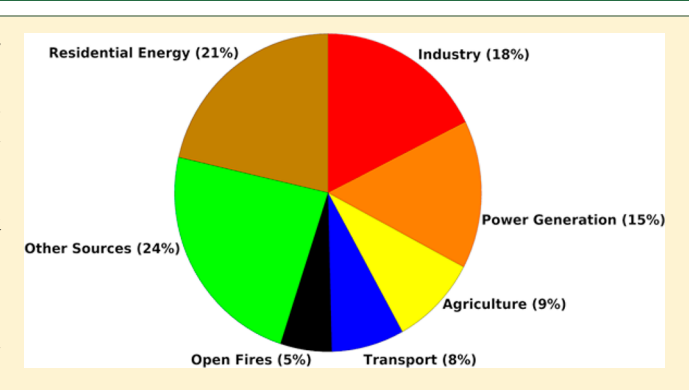
^uCenter for Environmental Science and Engineering, Indian Institute of Technology Kanpur, Kanpur, 208016, India ^vUNIDEF (CITEDEF-CONICET) Juan B. de la Salle 4397 – Villa Martelli, Buenos Aires B1603ALO, Argentina

^wDepartment of Chemistry, University of Dhaka, Dhaka 1000, Bangladesh

^xDepartment of Earth and Planetary Sciences, Weizmann Institute, Rehovot 76100, Israel

^ySchool of Population and Public Health, University of British Columbia, Vancouver, British Columbia V6T 1Z2, Canada

ABSTRACT: Exposure to ambient fine particulate matter $(PM_{2.5})$ is a leading risk factor for the global burden of disease. However, uncertainty remains about $PM_{2.5}$ sources. We use a global chemical transport model (GEOS-Chem) simulation for 2014, constrained by satellite-based estimates of $PM_{2.5}$ to interpret globally dispersed $PM_{2.5}$ mass and composition measurements from the ground-based surface particulate matter network (SPARTAN). Measured site mean $PM_{2.5}$ composition varies substantially for secondary inorganic aerosols $(2.4-19.7 \,\mu g/m^3)$, mineral dust $(1.9-14.7 \,\mu g/m^3)$, residual/organic matter $(2.1-40.2 \,\mu g/m^3)$, and black carbon $(1.0-7.3 \,\mu g/m^3)$. Interpretation of these measurements with the GEOS-Chem model yields insight into sources affecting each site. Globally, combustion



sectors such as residential energy use $(7.9 \,\mu\text{g/m}^3)$, industry $(6.5 \,\mu\text{g/m}^3)$, and power generation $(5.6 \,\mu\text{g/m}^3)$ are leading sources of outdoor global population-weighted PM_{2.5} concentrations. Global population-weighted organic mass is driven by the residential energy sector (64%) whereas population-weighted secondary inorganic concentrations arise primarily from industry (33%) and power generation (32%). Simulation-measurement biases for ammonium nitrate and dust identify uncertainty in agricultural and crustal sources. Interpretation of initial PM_{2.5} mass and composition measurements from SPARTAN with the GEOS-Chem model constrained by satellite-based PM_{2.5} provides insight into sources and processes that influence the global spatial variation in PM_{2.5} composition.

■ INTRODUCTION

Exposure to ambient fine particulate matter (PM_{2.5}; aerodynamic diameter of 2.5 µm or less) is a leading risk factor for increased mortality and morbidity. 1,2 The Global Burden of Disease study attributed 4.1 million premature deaths to PM_{2.5} exposure in 2016.3 A strong need exists to understand the sources contributing to this PM25 burden to inform mitigation efforts. PM_{2.5} formation is influenced by a range of emission sources, atmospheric transport, and atmospheric chemistry.⁵ A chemical transport model constrained by observations offers a powerful tool to understand these sources. Until recently, longterm measurements of PM_{2.5} mass and chemical composition were primarily limited to North America and Europe, with different networks using a variety of sampling techniques and standards to determine chemical composition. A global data set of ground-based PM_{2.5} compositional measurements could offer valuable information to understand the sources and processes that control the spatial diversity of PM_{2.5} mass and chemical

The relationship between emissions and PM_{2.5} loading is complex. PM_{2.5} can be emitted directly as particles from combustion or mechanical processes, but it can also form and grow in the atmosphere through the condensation of low volatility products of atmospheric chemical reactions of inorganic and organic precursors.^{5,6} Chemical transport models have been applied to represent this complexity through source apportionment studies aimed at characterizing the global sources contributing to PM_{2.5} mass and composition,⁷ with increasingly fine resolution.⁸ Although insightful, simulations could benefit from stronger observational constraints to evaluate and improve accuracy and spatial representativeness.

Two observational data sets have emerged recently with information about the global distribution of PM_{2.5} mass and composition, a dedicated ground-based network of PM_{2.5} composition, and increasingly accurate satellite-based estimates of PM_{2.5} mass. The surface particulate matter network (SPARTAN) measures ground-based PM_{2.5} mass and chemical composition using consistent instrumentation and standardized chemical analysis techniques in diverse global locations with high population densities relevant for health. Measurements from SPARTAN include PM_{2.5} filter samples that are analyzed

for PM $_{2.5}$ mass and chemical composition including sulfate, nitrate, ammonium, black carbon (BC), crustal material, and sea salt. 9,10 Satellite-based estimates of PM $_{2.5}$ mass complement the ground-based measurement network by offering additional global constraints on PM $_{2.5}$ mass at a resolution finer than global simulations. Case studies investigating the effects of model resolution on calculated PM $_{2.5}$ mortality rates find that those calculated from coarse (2° \times 2.5°) resolution are systematically lower than those calculated using finer (e.g., 0.5° \times 0.66°) resolution. 8,11,12 The latest global satellite-based PM $_{2.5}$ estimates combine observations from multiple retrieval algorithms $^{13-19}$ and instruments (MODIS, MISR, SeaWiFs) weighted inversely by error with respect to ground-based AOD measurements from AERONET 20 with additional statistical constraints from ground-based PM $_{2.5}$ measurements. $^{21-23}$

We apply the GEOS-Chem global chemical transport model, constrained by satellite-derived $PM_{2.5}$, to interpret ground-based measurements of $PM_{2.5}$ mass and composition from SPARTAN to gain insight into the main sources determining the spatial distribution of $PM_{2.5}$ mass and composition. We explore the annual average influence of major emission source categories on global population-weighted $PM_{2.5}$.

METHODS

SPARTAN Filter Measurements and Analysis. SPAR-TAN is an ongoing, long-term project that measures aerosol mass, water-soluble ions, trace elements, and aerosol optical properties at globally dispersed, densely populated areas of relevance to human health. Snider et al. 10 provide an overview of SPARTAN. Instrumentation includes an AirPhoton 3-wavelength integrating nephelometer and an AirPhoton SS4i filter sampler. We focus on the latter here. The PM_{2.5} is collected on a preweighed PTFE filter (2 μ m pore size, SKC). Filters sample one diurnal cycle over a 9-day period beginning and ending at 09:00 local time before shipment under ambient conditions to Dalhousie University for analysis in a central laboratory. Samples have been collected for periods of 2 months to over 3 years during 2013-2017 at 11 carefully chosen, regionally diverse sites. Although initially sparse, SPARTAN is unique in covering poorly sampled regions of the world with a consistent methodology.

An extensive overview of the SPARTAN PM25 sampling methodology, filter chemical analysis protocols, and the filterbased hygroscopicity parameter, κ , are provided by Snider et al.⁹ Details on relevant SPARTAN chemical analysis procedures and the uncertainty associated with each major chemical component based on collocated measurements is presented in the Supporting Information (SI). Seasonal mean uncertainties range from 4.0% for sulfate, to 4.6% for PM25, to 9.2% for nitrate. Briefly, gravimetric analysis follows USEPA protocols in a cleanroom with controlled temperature at 20-23 °C and relative humidity (RH) at 35 \pm 5%. Black carbon content is estimated by surface reflectance measurements, 24 water-soluble ions are determined by ion chromatography, 25 and trace elements are determined by inductively coupled plasma-mass spectrometry. 25,26 The residual matter (RM) component, estimated by subtracting the dry inorganic mass and particlebound water from total PM2.5 mass, is expected to be predominately organic.9 Activities are ongoing to directly measure organics through aerosol mass spectrometry²⁷ and Fourier transform infrared (FT-IR) spectroscopy.²⁸

GEOS-Chem Simulation. We use the GEOS-Chem 3-dimensional chemical transport model (v11.01, http://geoschem.org) to determine the daily distribution of PM25 major chemical component mass concentrations. GEOS-Chem solves for the evolution of atmospheric aerosols and gases using assimilated meteorology from the NASA Goddard Earth Observing System (GEOS), global and regional emission inventories, and algorithms that represent the physics and chemistry of atmospheric processes. The simulation uses assimilated meteorological observations (GEOS MERRA-2) at $2^{\circ} \times 2.5^{\circ}$ horizontal resolution with 47 vertical levels for the year 2014 for overlap with SPARTAN and due to emissions availability. The simulation uses anthropogenic emissions from the Emissions Database for Global Atmospheric Research (EDGAR) version 4.3 inventory²⁹ and the MIX regional anthropogenic emission inventory for 29 Asian regions and countries.3

SPARTAN measurements are used to inform developments to the simulation. We include the anthropogenic fugitive, combustion, and industrial dust (AFCID) emission inventory from Philip et al., 31 which increased correlation (r) with SPARTAN fine dust concentrations in this study from 0.35 to 0.67. Simulated total PM_{2.5} mass concentration is calculated at 35% RH for consistency with PM_{2.5} measurement protocols. The calculation employs the kappa hygroscopicity formulation³² used by SPARTAN, as described by Snider et al.; this formulation exhibits hygroscopic growth consistent with the aerosol inorganic model (AIM)³³ and laboratory measurements.⁹ Compared to the default GEOS-Chem model, the kappa hygroscopicity formulation decreases the bias (reduced major axis slope) of simulated PM_{2.5} versus SPARTAN PM_{2.5} concentrations from 1.39 to 1.29. We also include an aqueousphase mechanism for secondary organic aerosol (SOA) formation from isoprene from Marais et al.34 that better represents SPARTAN PM_{2.5} mass as shown by reduced root-mean-squareerror from 14.2 to 13.3 μ g/m³. We perform sensitivity simulations for which emissions from individual source categories were removed to calculate the contribution of sources to PM_{2.5} mass and composition by mass balance. Further details about the simulation are provided in the Supporting Information.

Constraining the Simulation with Satellite-Based PM_{2.5}. Satellite observations of AOD offer an additional constraint on the global PM_{2.5} distribution at spatial scales commensurate with population density distributions.³⁵ To reduce uncertainties in PM2.5 exposure estimates caused by model resolution, 8,36 satellite-derived PM_{2.5} concentrations²¹ for the year 2014 are used to downscale GEOS-Chem PM25 mass and composition from $2^{\circ} \times 2.5^{\circ}$ to $0.1^{\circ} \times 0.1^{\circ}$ resolution following a widely used approach.^{36–42} The spatial map of the annual ratio of satellite-derived to simulated PM_{2.5} concentration is applied to all simulated PM_{2.5} components, thus retaining the simulated fraction and temporal variation of PM_{2.5} composition.

Supplemental Table S2 shows the Pearson's correlation coefficient between SPARTAN measurements and PM_{2.5} components from the simulation (r) and simulated values scaled by local satellite-derived $PM_{2.5}$ (r_{sat}). For most $PM_{2.5}$ components, downscaling to satellite-derived PM_{2,5} increases the consistency in capturing PM_{2.5} spatial diversity. Correlations tend to increase, most notably for organic mass (OM, r_{sat} = 0.92 vs r = 0.64) as well as total PM_{2.5} mass ($r_{\text{sat}} = 0.93$ vs r =0.88), ammonium ($r_{\text{sat}} = 0.86 \text{ vs } r = 0.81$), and BC ($r_{\text{sat}} = 0.67 \text{ vs}$ r = 0.61). The root-mean-square-error of simulated total PM_{2.5} decreased from 13.3 $\mu g/m^3$ to 12.8 $\mu g/m^3$. Prior work has similarly found that the downscaled simulation better represents observations for both mass and composition. 36,41 Therefore, all values of total PM_{2.5} mass and chemical composition reported herein are from the downscaled simulation (scaled by the local annual ratio of PM_{2.5,sat} to PM_{2.5,model}) at $0.1^{\circ} \times 0.1^{\circ}$ resolution.

Sources Affecting PM_{2.5} Mass and Composition. Global Distribution of PM_{2.5} Chemical Composition. Figure 1 shows the annual mean simulated PM_{2.5} chemical composition with overlaid concentric circles depicting concentrations at SPAR-TAN sites. The center of each concentric circle indicates the measured value, with corresponding downscaled simulated concentration indicated by the outer ring. Differences between the outer ring and background map represent the effects of sampling the simulation for the same months as the measurements versus complete annual sampling. These seasonal sampling effects are generally much smaller than the global spatial variation, providing evidence of temporal representativeness. Inset values represent the global population-weighted mean concentration inferred from the downscaled simulation. Table 1 contains numerical values of measured and simulated concentrations for the specified sampling periods of SPARTAN sampling sites. The spatial variation of SPARTAN site-mean concentrations exceeds a factor of 5 (e.g., Kanpur, India vs Buenos Aires, Argentina) for most PM_{2.5} major chemical components, as described in more detail in the following sections.

SPARTAN measurements of secondary inorganic aerosol (SIA) vary by a factor of 8 across sampling sites from 2.4 μ g/m³ in Ilorin, Nigeria, to 19.7 μ g/m³ in Beijing, China, and account for over 20% of total PM_{2.5} mass at sampling sites, except Manila, Philippines (16%) and Ilorin (15%). The downscaled simulation captures the spatial heterogeneity of SIA concentrations (r = 0.87). SIA tends to be overestimated at SPARTAN sites, including an overestimate of nitrate concentrations in Beijing, as discussed below. SIA dominates population-weighted PM_{2.5}, accounting for 37% globally.

Measured concentrations of crustal material (dust) vary by an order of magnitude from $<2 \mu g/m^3$ (e.g., Buenos Aires) to $3-5 \mu g/m^3$ in many cities (e.g., Ilorin and Rehovot, Israel), to over 5 μg/m³ (Dhaka, Bangladesh; Hanoi, Vietnam; and Kanpur), and exceed 14 μ g/m³ in Beijing. Enhanced dust mass in Rehovot and Ilorin is expected to be predominately mineral dust, due to influence from the surrounding arid region. However, pronounced dust in urban cities throughout the South and Southeast Asia cannot be fully explained by mineral dust **Environmental Science & Technology**

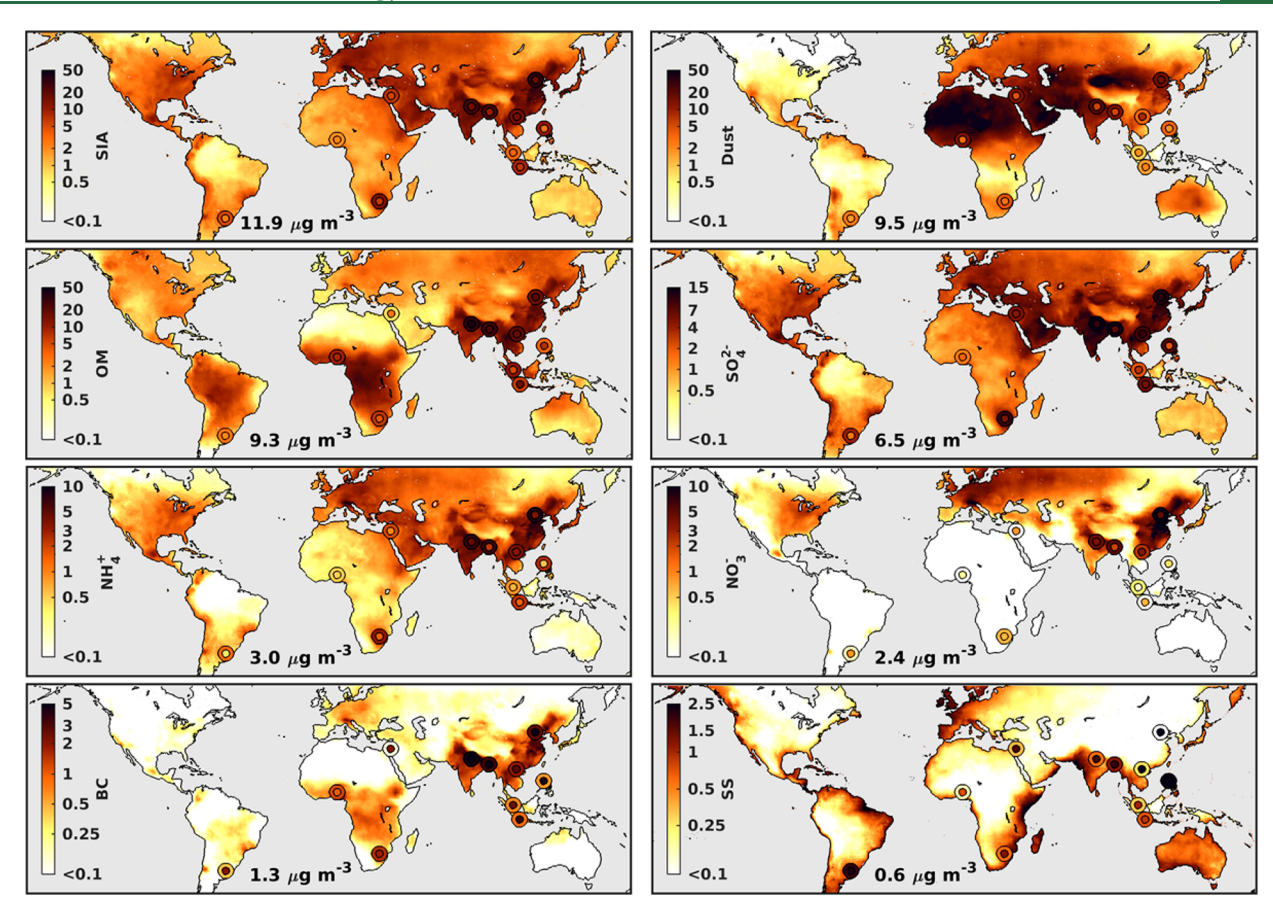


Figure 1. Global simulated annual mean PM_{2.5} composition. Values from SPARTAN observations are overlaid as colored circles surrounded by concentric circles showing simulated values sampled for consistent months. Concentrations are shown at 35% relative humidity. Abbreviations are secondary inorganic aerosol (SIA), organic mass (OM; residual mass from SPARTAN), black carbon (BC), and sea salt (SS). Inset values indicate global population-weighted average PM_{2.5} concentration resulting from each chemical component. Gray denotes water.

sources; elevated measured Zn:Al ratios at these sites⁹ suggest an anthropogenic component. The remaining positive bias in simulated values is driven by an overestimate in the simulated mineral dust source. Simulated dust concentrations are primarily mineral over the arid and semiarid regions of North Africa, the Middle East, and Central Asia, primarily AFCID in urban areas of Southeast Asia, and a combination of the two in Beijing. Dust contributes 29% to global population-weighted mean PM_{2.5} concentrations, making it the second largest global PM_{2.5} contributor.

As discussed in the methods, SPARTAN does not yet directly measure organic aerosol content; rather, the inferred residual matter (RM) is expected to be mainly organic, based on comparison with independent organic measurements. SPARTAN RM concentrations are highest throughout Asia where values exceeding 10 μ g/m³ are observed at all SPARTAN sites except Manila and Singapore. The lowest RM concentrations are found in Buenos Aires $(2.1 \,\mu\text{g/m}^3)$ and Rehovot $(2.7 \,\mu\text{g/m}^3)$. The broad consistency in spatial variation of SPARTAN RM and simulated OM (r = 0.92) provides supporting evidence that SPARTAN RM is dominated by organics. Simulated OM is enhanced over broad regions of South Asia, East Asia, and tropical Africa. Prior work has found that OM is a leading global PM_{2.5} chemical component for mean concentrations⁴¹ and trends.³⁶ We similarly find that OM continues to play a major role in populationweighted PM_{2.5}, following SIA and dust to contribute 28%.

Sulfate accounts for over 50% of SIA at all sampling sites, except Buenos Aires (46%), and accounts for approximately

6.5 μ g/m³ of population-weighted PM_{2.5} concentrations. SPARTAN measurements of sulfate concentrations exceed $5 \mu g/m^3$ at most sites in South and East Asia, in contrast with concentrations less than 2 μ g/m³ in Buenos Aires and Ilorin. The simulation generally captures the spatial distribution of measured sulfate concentrations (r = 0.78). Observations from the OMI satellite instrument have drawn attention to the pronounced SO₂ concentrations from coal combustion in East and South Asia, ⁴³ and sensitivity simulations have shown the influence of coal burning to the large PM_{2.5} burden over China.⁴⁴ The simulation reveals the spatial scale of the sulfate enhancement associated with these SO₂ sources. Modest measured enhancements are found in Rehovot, with associated regional scale enhancements across the Middle East. McLinden et al. 44 found evidence of missing SO₂ sources in the Middle East that could contribute to the regional sulfate burden. Low simulated concentrations across North America and Europe reflect the success of SO₂ emission controls over recent decades. 45-48

The spatial pattern of measured ammonium concentrations largely follows that of measured sulfate (r = 0.96) and nitrate (r = 0.93), associated with the formation of ammonium sulfate, ammonium bisulfate, and ammonium nitrate. Ammonium contributes less than 10% to measured PM_{2.5} concentrations with a population-weighted mean concentration of 3.0 μ g/m³. IASI satellite observations have revealed pronounced NH₃ enhancements across East and South Asia, ^{49,50} from agricultural systems. ⁵¹ Simulated ammonium concentrations are significantly correlated with measurements (r = 0.86), although

Table 1. PM_{2,5} Mass and Composition at SPARTAN Sites from Measurements (obs) and GEOS-Chem Simulation (GC). Values Are Reported in μ g m⁻³ for a Laboratory RH of 30-40%, and Simulated RH of 35%

			$PM_{2.5}$		SIA^a		SO_{4}^{2-}		NH_4^+	+	NO ₃ -		RM/OM ^b	2	dust		BC		sea salt ^d	Z.
site	lat/long (deg)	date range (mm/yyyy)	sqo	GC	sqo	gc	sqo	gc	sqo	gc	sqo	 25	sqo	l gc	sqo	gc	sqo	 25	sqo	GC
Beijing, China	40.01, 116.333	40.01, 116.333 06/2013-01/2017	67.1 ± 9.9^{e}	75.0	19.7 ± 2.1	36.3	11.2 ± 1.4	13.3	3.6 ± 0.6	0.6	$3.6 \pm 0.6 \ 9.0 \ 4.9 \pm 1.4$	4	21.9 ± 5.9	17.7	14.7 ± 2.4	17.9	$17.9 \ 7.3 \pm 2.1 \ 3.0$	3.0 3.	3.6 ± 0.8	0.1
Bandung, Indonesia	-6.888, 107.61	$-6.888, 107.61 01/2014 - 12/2016 30.8 \pm 4.5$	30.8 ± 4.5	20.0	7.6 ± 0.8	9.9	5.6 ± 0.7	7.2	$1.4 \pm 0.2 2.6$		0.6 ± 0.2	0.1	16.2 ± 4.4	6.8 2	2.2 ± 0.4	1.6	3.9 ± 1.1	6.0	0.9 ± 0.2	0.8
Manila, Philippines	14.635, 121.077	$14.635, 121.077 02/2014 - 01/2016 19.2 \pm 2.8$	19.2 ± 2.8	24.0	3.0 ± 0.3	12.0 2	2.1 ± 0.3	9.1	0.5 ± 0.1	2.9	0.4 ± 0.1	0.0	7.5 ± 2.0	3.7	1.9 ± 0.4	3.9	$4.3 \pm 1.2 0.6$		$2.5 \pm 0.6 3.8$	3.8
Rehovot, Israel	31.907, 34.81	02/2015-12/2016	17.5 ± 2.6	23.0	6.4 ± 0.7	7.7	4.7 ± 0.6	9.6	0.9 ± 0.1	2.0	0.8 ± 0.2	0.1	2.7 ± 0.7	0.7	4.6 ± 0.9	14.1	$2.1 \pm 0.6 0.1$		$1.7 \pm 0.4 0.4$	0.4
Dhaka, Bangladesh	23.728, 90.398	23.728, 90.398 10/2013-11/2015	49.9 ± 7.3	79.0	11.3 ± 1.1	28.0 7	7.1 ± 0.9	15.1	2.2 ± 0.4	7.2	2.0 ± 0.6	5.7	25.2 ± 6.8	30.2 5	5.5 ± 1.0	15.7	5.8 ± 1.7	3.7	2.0 ± 0.5	1.3
Buenos Aires, Argentina 34.556, -58.506 10/2014-10/2016	34.556, -58.506	10/2014-10/2016	10.7 ± 1.6	15.0	2.5 ± 0.3	6.2	1.3 ± 0.2	4.4	0.4 ± 0.1	1.5	0.4 ± 0.1 1.5 0.8 ± 0.2	0.3	2.1 ± 0.6	3.2	1.7 ± 0.3	2.8	$2.2 \pm 0.6 0.5$		2.3 ± 0.5	2.2
Ilorin, Nigeria	8.481, 4.526	03/2014-10/2015	15.8 ± 2.3	17.5	2.4 ± 0.2	1.9	1.7 ± 0.2	1.3 (0.5 ± 0.1	0.5	0.5 ± 0.1 $0.5 \pm 0.1 \pm 0.1$	0.1	8.4 ± 2.3	7.8 3	3.1 ± 0.6	6.4	$1.0\pm0.31.2$		$0.7\pm0.2\ 0.2$	0.2
Singapore, Singapore	1.298, 103.78	02/2016-02/2017	15.8 ± 2.3	15.6	4.0 ± 0.4	3.5 3	3.2 ± 0.4	2.2	0.6 ± 0.1	6.0	0.6 ± 0.1 0.9 0.2 \pm 0.1 0.4		5.2 ± 1.4	10.3	1.9 ± 0.4	6.0	$3.8 \pm 1.1 0.6$	0.6	$1.0 \pm 0.2 0.4$	0.4
Kanpur, India	26.519, 80.232	26.519, 80.232 12/2013-11/2014	71.9 ± 10.6	94.0	18.6 ± 1.9	29.2	10.2 ± 1.3		4.6 ± 0.8	9.7	$16.6 \ 4.6 \pm 0.8 \ 7.6 \ 3.8 \pm 1.1 \ 5.0$	5.0 40.	40.2 ± 10.9	35.5 5	5.6 ± 1.1	23.7	$5.6 \pm 1.6 \ 5.0 \ 1.8 \pm 0.4 \ 0.6$	5.0 1.	$.8 \pm 0.4$ (9.0
Hanoi, Vietnam	21.048, 105.801	$21.048, 105.801 \ 05/2015-03/2016 \ 50.9 \pm 7.5$	50.9 ± 7.5	45.0	$17.2 \pm 1.8 \ 17.1 \ 10.1 \pm 1.3$	17.1	10.1 ± 1.3		3.4 ± 0.6	4.5	$10.0 \ 3.4 \pm 0.6 \ 4.5 \ 3.7 \pm 1.1 \ 2.6$	2.6 17.	17.9 ± 4.9	21.7 8	$21.7 8.4 \pm 1.6$	3.7	$2.9 \pm 0.9 \ 2.1 \ 4.5 \pm 1.0 \ 0.3$	2.1 4.	5 ± 1.0	0.3
Pretoria, South Africa -25.757 , 28.279 $04/2016-06/2016$ 17.5 ± 2.6	-25.757, 28.279	04/2016-06/2016	17.5 ± 2.6	30.6	$30.6 7.3 \pm 0.7 15.7 5.3 \pm 0.7 11.3 1.4 \pm 0.2 3.7 0.6 \pm 0.2 0.7 4.3 \pm 1.2$	15.7	5.3 ± 0.7	11.3	1.4 ± 0.2	3.7	0.6 ± 0.2	0.7 4.3		7.5 2	7.5 2.8 ± 0.5		$5.1 1.8 \pm 0.5 1.7 1.3 \pm 0.3 0.7$	1.7 1.	3 ± 0.3	0.7
a SIA = secondary inorganic aerosol (sum of SO ₄ ²⁻ , NO ₃ ⁻ , and NH ₄ ⁺). b RM = residual matter, and OM = organic mass. c Dust from measurements calculated as $2.54[\text{Na}^{+}]_{\text{SS}}$ where $[\text{Na}^{+}]_{\text{sotal}}$ 0.1[Al]. c Values displayed after the \pm in the obs column represent the estimated seasonal uncertainty as described in the Sunnorting Information.	rganic aerosol (s ted as 2.54[Na ⁺	um of SO ₄ ²⁻ , NO ₃ -] _{SS} , where [Na ⁺] _{SS}	, and NH_4^+ = $[Na^+]_{total}$). ⁶ RM – 0.1[[= residual Al]. ^e Value	l matte s disp	er, and Ol layed aftε	M = or r the	ganic m ± in th	iass. ^c I e obs	Oust from column	measur	rements c it the est	alculat imated	ed as 10° I seasona	*([Al] 1 unce	+ [Mg] rtainty æ	+ [Fe] s descr). ^d SS fro	the
ark Lorento anno Adam																				

overestimated. Possible explanations of this overestimation include measurement artifacts, errors in thermodynamic predictions, and incomplete aerosol neutralization by organic inhibition of ammonia uptake not represented in the simulation, ^{52,53} as discussed further below and in the Supporting Information.

The degree of spatial variation in measured nitrate reflects the availability of nitric acid and excess ammonia to form ammonium nitrate. The highest measured concentrations are observed in Beijing (4.9 μ g/m³), Kanpur (3.8 μ g/m³), and Hanoi (3.7 μ g/m³), whereas the lowest are in Ilorin and Singapore (0.2 μ g/m³). The simulation generally reproduces the distribution of measured concentrations (r = 0.85); however, simulated concentrations are biased high in Beijing, Kanpur, and Dhaka where stronger agricultural ammonia sources exist. These discrepancies may reflect processes related to thermodynamic equilibrium between the gas and particle phase, aerosol neutralization as discussed in the Supporting Information, and uncertainty in NH₃ emissions.⁵⁴ It is also possible that semivolatile ammonium nitrate is lost from the filters despite the SPARTAN sampling procedure design to limit loss of semivolatile species such as ammonium nitrate, ¹⁰ and despite evidence of statistically insignificant trends in PM_{2.5} and ammonium nitrate mass when comparing the mass collected on the first sampled filter (54-day residence time in instrument) and the last filter sampled (negligible residence time).9 The simulated population-weighted mean nitrate concentration of 2.4 μ g/m³, driven by elevated concentrations in East Asia, South Asia, and Europe, may be overestimated.

BC concentrations vary by a factor of 7 across SPARTAN sites, with concentrations exceeding $5\,\mu g/m^3$ in Beijing ($7.3\,\mu g/m^3$), Dhaka ($5.8\,\mu g/m^3$), and Kanpur ($5.6\,\mu g/m^3$) and as low as $1.0\,\mu g/m^3$ in Ilorin. The GEOS-Chem simulation reveals the regional nature of the BC enhancements from a variety of combustion sources in East China and the Indo-Gangetic Plain. The downscaled simulation generally captures the BC concentrations at most SPARTAN sites (r=0.67), suggesting skill in capturing the heterogeneous sources of this primary PM_{2.5} component at the global scale. Population-weighted mean BC concentration is an order of magnitude lower than SIA at 4%.

Sea salt concentrations are low in both the measurements and simulation, yielding a contribution to population-weighted $PM_{2.5}$ of less than 2%.

SPARTAN Site Characteristics. SPARTAN composition measurements also offer insight into the site-specific source attribution from sensitivity simulations. The downscaled simulation generally captures the global spatial heterogeneity of major chemical components measured by SPARTAN as summarized in Table S2. Below, we use sensitivity simulations as described in the SI to further interpret SPARTAN measurements of PM_{2.5} mass and chemical composition to understand sources in regions traditionally underrepresented by measurements of PM_{2.5} components. Source categories selected for investigation follow those of Lelieveld et al. as described in Table S3. The presentation is grouped by region, the left column of all Figures S3-S8 shows measured PM25 composition at the indicated SPARTAN site. The simulated chemical composition summed across all source sectors (Sens. Sim.) can exceed the downscaled simulated chemical composition (Sim.) due to nonlinearity in aerosol processes, primarily affecting nitrate, ammonium, and SOA. The agricultural source is most strongly influenced by this process and is likely overestimated both here and in other studies that exclude specific sources.

East Asia. Figure S3 shows the measured PM_{2.5} composition and source attribution at two SPARTAN sites located in East Asia: Hanoi, Vietnam and Beijing, China. Measured PM25 composition is dominated by RM (likely OM), followed by dust and sulfate. Residential energy use dominates the OM component of PM2.5 through the burning of solid fuels for domestic cooking, space heating, and industrial purposes.⁵⁵ Bonjour et al. se estimate approximately 50% of the 2010 population in Vietnam and China burned solid fuels for domestic use. Open fires and other sources also contribute to OM in Hanoi due to transport of seasonal biomass burning plumes from Southeast Asia and the oxidation of biogenic volatile organic compounds (VOCs). SPARTAN measurements indicate that dust accounts for 22% of PM_{2.5} in Beijing and 17% in Hanoi. In Beijing we find contributions from both mineral and anthropogenic dust, consistent with prior work. 9,31,57 Simulated dust concentrations in Hanoi are driven by urban sources and underestimate the observations. Sulfate concentrations are influenced primarily by emissions from industry and power generation. Numerous studies have reported that decreasing SO₂ emissions from power generation in East Asia are being partially offset by rising SO₂ emissions from industrial activity. 55,58,59 Ma et al. 40 estimate that coal combustion contributes to 40% of the total PM_{2.5} in Chinese cities. Ammonium concentrations are mostly from agricultural NH3 and affected by formation with sulfate and nitrate. Agricultural activity has the largest impact on nitrate concentrations due to the limiting role that ammonia can play in ammonium nitrate formation. 6,60,61 The positive bias in simulated nitrate and ammonium in Beijing could reflect loss of semivolatile species from measurements, errors in simulated thermodynamic partitioning, or missing processes. 53,62 The bias is exacerbated by the sensitivity simulations due to nonlinear chemistry, when excluding specific sources, likely leading to an overestimate of the role of agriculture. Hanoi exhibits a minor increase in OM when emissions from agriculture are removed due to increased aerosol acidity, as this ammonia source neutralizes acidic components. Industrial sources of NO_x (NO + NO₂) also contribute to nitrate formation in East Asia. 50,61 BC has two primary source categories: residential energy and industrial activity; the negative bias could reflect heterogeneity of this primary source. Overall, each of the investigated source categories are active in East Asia and contribute to the complex PM_{2.5} mixture measured by SPARTAN.

South Asia. Figure S4 shows the measured PM25 composition and source attribution at two SPARTAN sites located in South Asia: Kanpur, India, and Dhaka, Bangladesh. Overall consistency is found across the two simulated source attributions. Kanpur is situated in the Indo-Gangetic plain where significant agricultural and industrial activity occur^{63,64} and stagnant air in winter enhances particulate matter concentrations. 65-67 Dhaka is influenced by air masses transported from the Indo-Gangetic plain⁶⁸ as well as strong local emission sources. The residential energy use source category is the largest simulated contributor to PM25 in Kanpur and Dhaka, by substantially influencing OM and BC. An estimated 58% of the population in India and 91% of the population in Bangladesh in 2010 burned solid fuels for domestic heating and cooking. So Sulfate concentrations are most heavily influenced by the power generation and industry source categories. Generally, there has been an increase in SO₂ emissions from India, driven by rapid economic development. Fioletov et al. found that coalfired power plants account for nearly all major SO2 emission

sources seen by the OMI spacecraft instrument in India, with growth of a factor of 2 over 2005–2014, and a factor of 3 in the Chhattisgarh and Odisha regions, located south of the Kanpur site and west of the Dhaka site. The main fuel for the iron and steel industry is coal, resulting in SO₂ emissions from this sector as well. 55,58 Current legislation does not require the installation of fuel gas desulfurization in either the industrial or power generation sectors. 43,58 Elevated observed ammonia concentrations⁴⁹ contribute to measured ammonium sulfate, and the sensitivity of ammonium to emissions from industry and power generation. Dust is a notable contributor to measured PM_{2.5} in South Asia, accounting for 11% of total PM_{2.5} in Dhaka and 8% in Kanpur due to both anthropogenic and natural sources. Previous studies (e.g., refs 63,71-76) have found evidence of desert dust transport from the western Thar Desert, Northeast Africa, and the Gulf region. The overestimation of the dust contribution to PM_{2.5} by the simulation highlights the need for further development of the AFCID inventory and mineral dust simulation.

Southeast Asia. Figure S5 shows the measured PM_{2.5} composition and source attribution at three SPARTAN sites in Southeast Asia: Bandung, Indonesia; Manila, Philippines; and Singapore. At all three sites, measured PM_{2.5} is dominated by RM/OM, sulfate, and BC. The residential energy use source category has the largest impact on OM concentrations in Bandung and Manila through the burning of solid fuels in domestic cooking and heating; at least 50% of the population in Indonesia and the Philippines was estimated to burn solid fuels for domestic cooking in 2010. 56 The negative biases in simulated OM and BC contributions suggest the contribution from the residential energy use combustion source may be underestimated. Open fires dominate OM concentrations in Singapore where seasonal biomass burning events throughout Southeast Asia significantly impact ground-level air quality. 77-79 The OM simulation bias in Singapore could reflect mismatch in representing long-range transport of biomass burning emissions for the measurement period. Significant contributions to sulfate concentrations arise from the industry and power generation source categories from SO₂ emissions due to burning of highsulfur containing fossil fuels in boilers, limestone kilns, furnaces, and power plants. A minor source of sulfate is the other source category as atmospheric oxidation of oceanic DMS, 80 and in Bandung, nearby volcanos. 81 The overestimation of sulfate and ammonium in Manila, which is not found at the other two sites in this region, implies uncertainty in local emissions. The low measured and simulated nitrate concentrations at all three sites reflect ambient temperatures that thermodynamically limit NH₄NO₃ formation. The dust component of PM_{2.5} in Southeast Asia is dominated by anthropogenic dust from industry, power generation, and transport in this region.

Sub-Saharan Africa. Figure S6 shows the measured $PM_{2.5}$ composition and source attribution in Ilorin, Nigeria, and Pretoria, South Africa. Both sites have measured $PM_{2.5}$ concentrations below 20 μ g m⁻³ that are mostly composed of residual (organic) mass, dust, and sulfate. Pronounced mineral dust concentrations in Ilorin arise from the Sahara Desert, where seasonal Harmattan trade winds advect fine dust to West Africa. Both sites are influenced by the open fires and residential energy use source categories. Ilorin is downwind of seasonal biomass burning events in west Africa, whereas open fires in central Africa affect South Africa. The burning of solid fuels (e.g., biofuel and coal) for domestic stoves and heaters accounts for the influence of the residential energy category on

Environmental Science & Technology

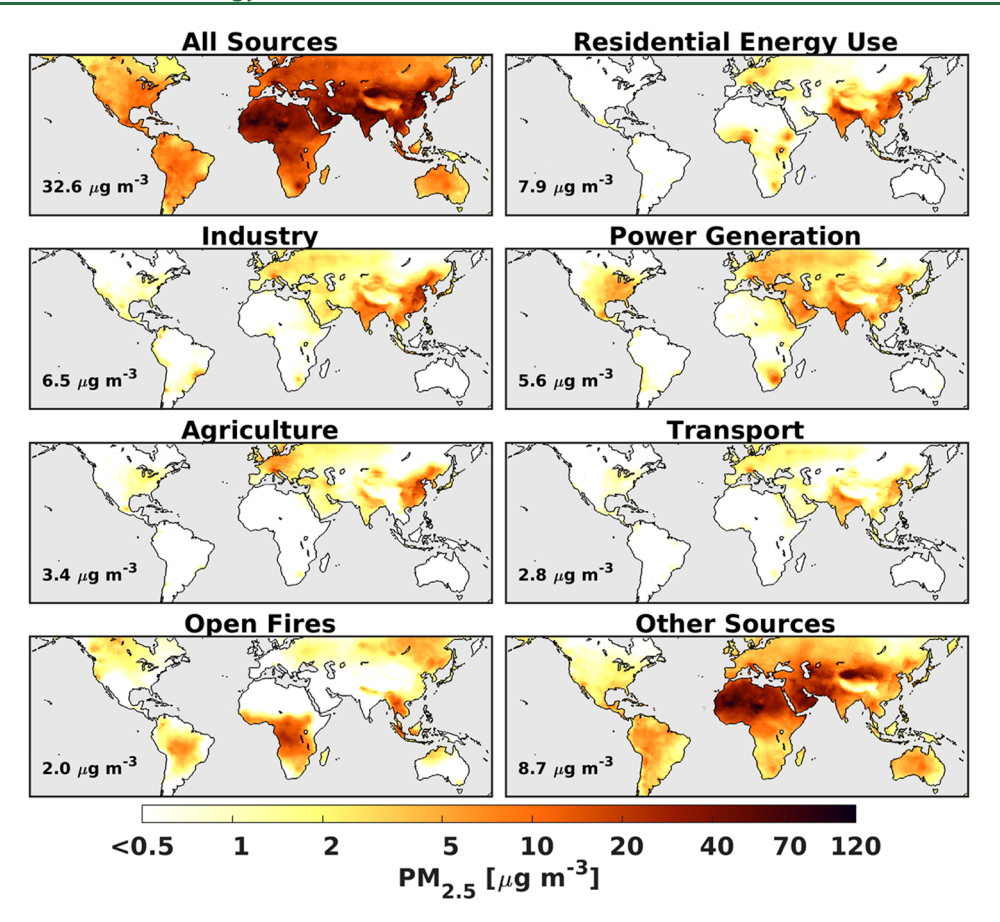


Figure 2. Global simulated annual mean total $PM_{2.5}$ mass (top left) and contribution from seven source categories at 35% RH following measurement protocols. Inset values display the global population-weighted average $PM_{2.5}$ concentration from each source category. Gray denotes water.

organic, sulfate, and BC concentrations. In 2010 an estimated 74% of households used solid fuels for domestic cooking in Nigeria. 56 Other sources of OM in $PM_{2.5}$ are biogenic VOCs from regional vegetation. Unlike many other SPARTAN sites, the industry and power generation source categories have minimal influence on $PM_{2.5}$ concentrations in Ilorin. However, power generation and industry are leading contributing source categories to sulfate in the industrialized city of Pretoria, although uncertainty in these emissions may lead to an overestimation.

Buenos Aires, Argentina. Figure S7 shows the measured PM_{2.5} composition and source attribution in Buenos Aires, Argentina. Distinct from other SPARTAN sites, sensitivity simulations suggest most PM2.5 arises from other, mostly natural, sources. SPARTAN measurements corroborate this conclusion, with 21% of PM_{2.5} from sea salt, 20% from organics, and 16% from mineral dust. Mineral dust from the arid desert region to the northwest of the city influences the dust content of PM_{2.5} at this site.⁷³ Substantial cropland to the west and tree covered areas to the north⁸⁴ provide a source of secondary organic aerosol from oxidation of biogenic emissions of VOCs such as isoprene and other monoterpenes. The flux of oceanic DMS influences sulfate; 80 however, this source appears overestimated as indicated by the measurement-simulation differences. Industry and power generation are also notable sources of sulfate in Buenos Aires. Open fires from deforestation activity in the Amazon produce plumes that affect air quality in Argentina. Organic content increases when ammonia emissions from agriculture are removed due to increased aerosol acidity.

Rehovot, Israel. Figure S8 shows the measured PM25 composition and source attribution at the Middle East site in Rehovot, Israel. Other, mostly natural, sources are the leading source category in this region, dominated by mineral dust; SPARTAN measurements indicate that 26% of PM_{2.5} is dust, and also suggest that the simulation is overestimating this source. Power generation has the largest anthropogenic impact on PM_{2.5} concentrations and is the leading source of sulfate at this site. The Middle East is among the largest SO₂ emitting regions in the world from oil fields and refineries. 43,44,7 Transport of air masses from Europe have been shown to influence ground-level concentrations (e.g., refs 87, 88). Ammonium is found to be sensitive to sources of sulfate, suggesting elevated background NH₃; Clarisse et al. 49 reported NH₃ columns well above background level in the Nile River Delta, southwest of the sampling site. Simulated ammonium is again higher than measurements. Elevated temperatures thermodynamically inhibit formation of particulate nitrate. The negative bias in simulated OM and BC suggests a missing combustion source.

Global $PM_{2.5}$ Source Categories. Overall, the general consistency of the simulation with measured $PM_{2.5}$ composition supports the applicability of using sensitivity simulations to explore the influence of source categories to global population-weighted $PM_{2.5}$. The most prominent exceptions are positive bias in ammonium nitrate and dust, implying that sensitivities to agricultural and crustal sources should be interpreted with caution. Figure 2 shows the impact of seven source categories to $PM_{2.5}$ as determined from sensitivity simulations that separately exclude each source. Values inset show the global population-weighted mean $PM_{2.5}$ concentrations from each source. The sum

of PM_{2.5} concentrations from the seven source sectors exceeds the global mean PM_{2.5} concentration (36.9 vs 32.6 μ g/m³) due to nonlinearity in modeled aerosol processes.

Six primarily anthropogenic categories contribute 76% of global $PM_{2.5}$ exposure. The residential energy use sector has the largest anthropogenic contribution, responsible for 21% (7.9 $\mu g/m^3$) of population-weighted $PM_{2.5}$. This residential category primarily includes small combustion sources for domestic heating, cooking, and waste disposal. These biofuel sources, diesel generators and burning of household waste, produce a large amount of indoor and outdoor carbonaceous $PM_{2.5}$ with implications for human health. The contribution of this source category to outdoor $PM_{2.5}$ is most pronounced in the populous areas of South Asia, East Asia, and Africa. Lacey et al. Found that the elimination of solid fuel cookstoves over a 20-year period could avoid 22.5 million premature deaths associated with outdoor $PM_{2.5}$ between the years 2000 and 2100.

Industry is the second largest anthropogenic source category, contributing to 18% (6.5 μ g/m³) of population-weighted PM_{2.5}. Emissions from the industry source category include manufacturing of iron, steel, pulp, and paper, as well as oil refineries and fuel production. Industry contributes significantly to PM_{2.5} in China and India and has a notable impact near major urban areas in the Americas, Europe, and Southeast Asia. The impact is highest in emerging economies and industrialized countries, in part due to international trade.

The four remaining anthropogenic categories are responsible for 37% of population-weighted PM_{2.5}. Power generation, although not the leading source in any one region, makes a prominent contribution of 15% to global population-weighted PM_{2.5}. Emissions of SO₂ and NO_x from fossil fuel fired power plants are readily oxidized in the atmosphere to sulfate and nitrate, leading to enhanced PM_{2.5} concentrations, especially in South Asia, East Asia, and North America. Agriculture, primarily NH₃ and NO_x from fertilizer and domesticated animals, contributes 9% to global-population weighted PM_{2.5}. Agriculture is the leading source category in most of Europe and one of the leading sources over much of China and parts of India, similar to the findings of Lelieveld et al. The PM_{2.5} contribution from agricultural activity is largest where both a large nitric acid burden exists from NO_x emissions and where excess ammonia is available. The positive biases found in simulated ammonium nitrate suggest the sensitivity of PM_{2.5} to this source may be overestimated. Transportation emissions contribute 8% of global population-weighted PM_{2.5} through emissions of NO_x, organics, BC, and SO₂; the most heavily influenced regions are East Asia, Southeast Asia, and the Indo-Gangetic plain. Emissions of carbonaceous aerosol and gaseous organic compounds from open fires comprise only 5% of population-weighted mean PM_{2.5} concentrations. However, open fires can dominate PM_{2.5} mass in large parts of the tropical and borealforests.

All sources not clearly controlled by mitigation strategies, primarily natural in origin, are lumped into a single "Other sources" category described in Table S3. This combined Other category contributes 24% of population-weighted $PM_{2.5}$. Sources include mineral dust that dominates $PM_{2.5}$ in arid and semiarid regions of North Africa, the Middle East, Central Asia, and Australia. The size distribution of lofted dust aerosols extends from the coarse mode into the fine mode of $PM_{2.5}$ that can remain suspended and undergo long-range transport. ^{93,94} This dust source may be overestimated. Sources of biogenic organic compounds, NO_x from soil, and microbial activity

of oceanic dimethyl sulfide contribute to a diffuse $PM_{2.5}$ background.

DISCUSSION

This initial interpretation of globally dispersed ambient $PM_{2.5}$ mass and composition measurements from SPARTAN with the GEOS-Chem model, with development motivated by SPARTAN measurements and constrained by satellite-based estimates of $PM_{2.5}$, identified a promising level of agreement along with areas for further model development. To our knowledge, this is the first global source attribution study that includes either constraints from satellite observations or comparison with global $PM_{2.5}$ composition measurements. Consistency between simulated and observed $PM_{2.5}$ composition adds confidence in utilizing the sensitivity simulations to identify the ambient $PM_{2.5}$ sources with prominent influence on population-weighted $PM_{2.5}$. The pronounced global contributions from residential energy use (21%), industry (18%), and power generation (15%) warrant further attention.

However, site-specific discrepancies between measured and simulated components such as nitrate/ammonium in Beijing and Kanpur, sulfate/ammonium in Manila and Buenos Aires, and dust in Ilorin and Rehovot provide insight into local biases in simulated PM_{2.5} composition. It is possible that previous global source attribution studies (e.g., refs 7, 95, and 96) exhibit biases as well. Evidence of incomplete sulfate neutralization at SPARTAN sites, which is not captured in the simulation, requires additional investigation as this may partially explain the overestimate of simulated ammonium and nitrate concentrations. Although improvements to the dust simulation and emissions have been implemented in recent model versions (e.g., refs 31, 97), further attention is needed to mineral and AFCID emission inventories to address regional differences. 98 Simulated OM remains underestimated at most SPARTAN sites, reiterating that development is needed to aerosol processes (e.g., SOA formation) and emission inventories that control this primary component (e.g., residential energy use and open fires). SPARTAN provides speciated PM_{2.5} measurements in many traditionally under-sampled regions, which could be used to constrain assimilations and inform developments to global chemical transport models. Additional ground-based, global measurements of PM_{2.5} mass and composition will also be important to evaluate and improve these source attribution estimates.

We welcome expressions of interest to join this grass-roots network. Data collected by SPARTAN are publicly available at www.spartan-network.org.

ASSOCIATED CONTENT

S Supporting Information

The Supporting Information is available free of charge on the ACS Publications website at DOI: 10.1021/acs.est.8b01658.

Detailed description of SPARTAN chemical composition measurements and uncertainty estimates based on collocated measurements, GEOS-Chem simulation, and extent of sulfate neutralization; supporting figures for the site characteristics section (PDF)

AUTHOR INFORMATION

Corresponding Author

*Phone: 902-494-1820; fax: 902-494-5191; e-mail: Crystal. Weagle@Dal.ca.

ORCID ®

Crystal L. Weagle: 0000-0002-7705-9604

Chi Li: 0000-0002-8992-7026 Yang Liu: 0000-0001-5477-2186 Eloise A. Marais: 0000-0001-5477-8051 Sachchida N. Tripathi: 0000-0002-6402-4680 Michael Brauer: 0000-0002-9103-9343 Yinon Rudich: 0000-0003-3149-0201

Notes

The authors declare no competing financial interest.

ACKNOWLEDGMENTS

SPARTAN is an IGAC-endorsed activity (www.igacproject. org). The National Sciences and Engineering Research Council of Canada supported this work. Crystal Weagle was partially supported by the Nova Scotia Research and Innovation Graduate Scholarship. Sachchida Tripathi acknowledges the Indo-UK joint project (Grant no. DST/INT/UK/P-144/2016), UKIERI, and is thankful to DST for the financial support. Yinon Rudich acknowledges support from the Israel Science Foundation (Grant No. 236/16) and from the Environmental Health Fund (Israel). We are grateful to the numerous SPARTAN site operators for their careful measurements presented here.

■ REFERENCES

- (1) Dockery, D. W.; Pope, C. A.; Xiping, X.; Spengler, J. D.; Ware, J. H.; Fay, M. E.; Ferris, B. G.; Speizer, F. E. An Association Between Air Pollution and Mortality in Six U.S. Cities. *N. Engl. J. Med.* **1993**, 329 (24), 1753–1759.
- (2) Pope, C. A.; Ezzati, M.; Dockery, D. W. Fine-Particulate Air Pollution and Life Expectancy in the United States. *N. Engl. J. Med.* **2009**, 360 (4), 376–386.
- (3) GBD 2016 Risk Factors Collaborators. Global, Regional, and National Comparative Risk Assessment of 84 Behavioural, Environmental and Occupational, and Metabolic Risks or Clusters of Risks, 1990–2016: A Systematic Analysis for the Global Burden of Disease Study 2016. *Lancet* 2017, 390 (10100), 1345–1422.
- (4) West, J. J.; Cohen, A.; Dentener, F.; Brunekreef, B.; Zhu, T.; Armstrong, B.; Bell, M. L.; Brauer, M.; Carmichael, G.; Costa, D. L.; Dockery, D. W.; Kleeman, M.; Krzyzanowski, M.; Künzli, N.; Liousse, C.; Lung, S. C. C.; Martin, R. V.; Pöschl, U.; Pope, C. A.; Roberts, J. M.; Russell, A. G.; Wiedinmyer, C. What We Breathe Impacts Our Health: Improving Understanding of the Link between Air Pollution and Health. *Environ. Sci. Technol.* **2016**, *50* (10), 4895–4904.
- (5) Fuzzi, S.; Baltensperger, U.; Carslaw, K.; Decesari, S.; Denier Van Der Gon, H.; Facchini, M. C.; Fowler, D.; Koren, I.; Langford, B.; Lohmann, U.; Nemitz, E.; Pandis, S.; Riipinen, I.; Rudich, Y.; Schaap, M.; Slowik, J. G.; Spracklen, D. V.; Vignati, E.; Wild, M.; Williams, M.; Gilardoni, S. Particulate Matter, Air Quality and Climate: Lessons Learned and Future Needs. *Atmos. Chem. Phys.* **2015**, *15* (14), 8217–8299.
- (6) Pandis, S. N.; Wexler, A. S.; Seinfeld, J. H. Dynamics of Tropospheric Aerosols. J. Phys. Chem. 1995, 99 (24), 9646–9659.
- (7) Lelieveld, J.; Evans, J. S.; Fnais, M.; Giannadaki, D.; Pozzer, A. The Contribution of Outdoor Air Pollution Sources to Premature Mortality on a Global Scale. *Nature* **2015**, *525* (7569), 367–371.
- (8) Punger, E. M.; West, J. J. The Effect of Grid Resolution on Estimates of the Burden of Ozone and Fine Particulate Matter on Premature Mortality in the USA. *Air Qual., Atmos. Health* **2013**, *6*, 563–573.
- (9) Snider, G.; Weagle, C. L.; Murdymootoo, K. K.; Ring, A.; Ritchie, Y.; Stone, E.; Walsh, A.; Akoshile, C.; Anh, N. X.; Balasubramanian, R.; Brook, J.; Qonitan, F. D.; Dong, J.; Griffith, D.; He, K.; Holben, B. N.; Kahn, R.; Lagrosas, N.; Lestari, P.; Ma, Z.; Misra, A.; Norford, L. K.;

- Quel, E. J.; Salam, A.; Schichtel, B.; Segev, L.; Tripathi, S.; Wang, C.; Yu, C.; Zhang, Q.; Zhang, Y.; Brauer, M.; Cohen, A.; Gibson, M. D.; Liu, Y.; Martins, J. V.; Rudich, Y.; Martin, R. V. Variation in Global Chemical Composition of PM_{2.5}Emerging Results from SPARTAN. *Atmos. Chem. Phys.* **2016**, *16* (15), 9629–9653.
- (10) Snider, G.; Weagle, C. L.; Martin, R. V.; vanDonkelaar, A.; Conrad, K.; Cunningham, D.; Gordon, C.; Zwicker, M.; Akoshile, C.; Artaxo, P.; Anh, N. X.; Brook, J.; Dong, J.; Garland, R. M.; Greenwald, R.; Griffith, D.; He, K.; Holben, B. N.; Kahn, R.; Koren, I.; Lagrosas, N.; Lestari, P.; Ma, Z.; VanderleiMartins, J.; Quel, E. J.; Rudich, Y.; Salam, A.; Tripathi, S. N.; Yu, C.; Zhang, Q.; Zhang, Y.; Brauer, M.; Cohen, A.; Gibson, M. D.; Liu, Y. SPARTAN: A Global Network to Evaluate and Enhance Satellite-Based Estimates of Ground-Level Particulate Matter for Global Health Applications. *Atmos. Meas. Tech.* **2015**, *8*, 505–521.
- (11) Li, Y.; Henze, D. K.; Jack, D.; Kinney, P. L. The Influence of Air Quality Model Resolution on Health Impact Assessment for Fine Particulate Matter and Its Components. *Air Qual., Atmos. Health* **2016**, 9 (1), 51–68.
- (12) Kodros, J. K.; Wiedinmyer, C.; Ford, B.; Cucinotta, R.; Gan, R.; Magzamen, S.; Pierce, J. R. Global Burden of Mortalities Due to Chronic Exposure to Ambient PM_{2.5} from Open Combustion of Domestic Waste. *Environ. Res. Lett.* **2016**, *11*, 124022.
- (13) Hsu, N. C.; Tsay, S. C.; King, M. D.; Herman, J. R. Deep Blue Retrievals of Asian Aerosol Properties during ACE-Asia. *IEEE Trans. Geosci. Remote Sens.* **2006**, 44 (11), 3180–3195.
- (14) Levy, R. C.; Remer, L. A.; Mattoo, S.; Vermote, E. F.; Kaufman, Y. J. Second-Generation Operational Algorithm: Retrieval of Aerosol Properties over Land from Inversion of Moderate Resolution Imaging Spectroradiometer Spectral Reflectance. *J. Geophys. Res. Atmos.* **2007**, *112* (13), 1–21.
- (15) Martonchik, J. V.; Kahn, R. a; Diner, D. J. Retrieval of Aerosol Properties over Land Using MISR Observations. In *Satellite Aerosol Remote Sensing over Land*; Springer: 2009; pp 267–293.
- (16) Lyapustin, A.; Martonchik, J.; Wang, Y.; Laszlo, I.; Korkin, S. Multiangle Implementation of Atmospheric Correction (MAIAC): 1. Radiative Transfer Basis and Look-up Tables. *J. Geophys. Res.* **2011**, *116* (3), No. 14985, DOI: 10.1029/2010JD014985.
- (17) Lyapustin, A.; Wang, Y.; Laszlo, I.; Kahn, R.; Korkin, S.; Remer, L.; Levy, R.; Reid, J. S. Multiangle Implementation of Atmospheric Correction (MAIAC): 2. Aerosol Algorithm. *J. Geophys. Res.* **2011**, *116* (3), No. 14986, DOI: 10.1029/2010JD014986.
- (18) Hsu, N. C.; Jeong, M. J.; Bettenhausen, C.; Sayer, A. M.; Hansell, R.; Seftor, C. S.; Huang, J.; Tsay, S. C. Enhanced Deep Blue Aerosol Retrieval Algorithm: The Second Generation. *J. Geophys. Res. Atmos.* **2013**, *118* (16), 9296–9315.
- (19) Levy, R. C.; Mattoo, S.; Munchak, L. A.; Remer, L. A.; Sayer, A. M.; Patadia, F.; Hsu, N. C. The Collection 6 MODIS Aerosol Products over Land and Ocean. *Atmos. Meas. Tech.* **2013**, *6* (11), 2989–3034.
- (20) Holben, B. N.; Eck, T. F.; Slutsker, I.; Tanre, D.; Buis, J.; Setzer, A.; Vermote, E.; Reagan, J. A.; Kaufman, Y. J.; Nakajima, T.; Lavenu, F.; Jankowiak, I.; Smirnov, A. AERONET A Federated Instrument Network and Data Archive for Aerosol Characterization. *Remote Sens. Environ.* 1998, 4257 (66), 1–16.
- (21) van Donkelaar, A.; Martin, R. V.; Brauer, M.; Hsu, N. C.; Kahn, R. A.; Levy, R. C.; Lyapustin, A.; Sayer, A. M.; Winker, D. M. Global Estimates of Fine Particulate Matter Using a Combined Geophysical-Statistical Method with Information from Satellites, Models, and Monitors. *Environ. Sci. Technol.* **2016**, *50*, 3762–3772.
- (22) Shaddick, G.; Thomas, M. L.; Green, A.; Brauer, M.; vanDonkelaar, A.; Burnett, R.; Chang, H. H.; Cohen, A.; vanDingenen, R.; Dora, C.; Gumy, S.; Liu, Y.; Martin, R.; Waller, L. A.; West, J.; Zidek, J. V.; Prüss-Ustün, A. Data Integration Model for Air Quality: A Hierarchical Approach to the Global Estimation of Exposures to Ambient Air Pollution. *J. R. Stat. Soc. Ser. C Appl. Stat.* **2018**, *67*, 231–253.
- (23) Shaddick, G.; Thomas, M.; Amini, H.; Broday, D. M.; Cohen, A.; Frostad, J.; Green, A.; Gumy, S.; Liu, Y.; Martin, R. V.; Prüss-Üstün, A.; Simpson, D.; vanDonkelaar, A.; Brauer, M. Data Integration for the Assessment of Population Exposure to Ambient Air Pollution for

- Global Burden of Disease Assessment. Environ. Sci. Technol. 2018, 52,
- (24) Quincey, P.; Butterfield, D.; Green, D.; Coyle, M.; Cape, N. J. An Evaluation of Measurement Methods for Organic, Elemental and Black Carbon in Ambient Air Monitoring Sites. Atmos. Environ. 2009, 43 (32), 5085-5091.
- (25) Gibson, M. D.; Heal, M. R.; Li, Z.; Kuchta, J.; King, G. H.; Hayes, A.; Lambert, S. The Spatial and Seasonal Variation of Nitrogen Dioxide and Sulfur Dioxide in Cape Breton Highlands National Park, Canada, and the Association with Lichen Abundance. Atmos. Environ. 2013, 64, 303-311
- (26) Gibson, M. D.; Pierce, J. R.; Waugh, D.; Kuchta, J.; Chisholm, L.; Duck, T. J.; Hopper, J. T.; Beauchamp, S.; King, G. H.; Franklin, J. E.; Leaitch, W. R.; Wheeler, A. J.; Li, Z.; Gagnon, G. A.; Palmer, P. I. Identifying the Sources Driving Observed PM_{2.5} Temporal Variability over Halifax, Nova Scotia, during BORTAS-B. Atmos. Chem. Phys. **2013**, 13 (1), 1–13.
- (27) Daellenbach, K. R.; Bozzetti, C.; Křepelová, A.; Canonaco, F.; Wolf, R.; Zotter, P.; Fermo, P.; Crippa, M.; Slowik, J. G.; Sosedova, Y.; Zhang, Y.; Huang, R. J.; Poulain, L.; Szidat, S.; Baltensperger, U.; ElHaddad, I.; Prévôt, A. S. H. Characterization and Source Apportionment of Organic Aerosol Using Offline Aerosol Mass Spectrometry. Atmos. Meas. Tech. 2016, 9 (1), 23-39.
- (28) Weakley, A. T.; Takahama, S.; Dillner, A. M. Ambient Aerosol Composition by Infrared Spectroscopy and Partial Least-Squares in the Chemical Speciation Network: Organic Carbon with Functional Group Identification. Aerosol Sci. Technol. 2016, 50 (10), 1096-1114.
- (29) Crippa, M.; Janssens-Maenhout, G.; Dentener, F.; Guizzardi, D.; Sindelarova, K.; Muntean, M.; vanDingenen, R.; Granier, C. Forty Years of Improvements in European Air Quality: Regional Policy-Industry Interactions with Global Impacts. Atmos. Chem. Phys. 2016, 16 (6), 3825 - 3841.
- (30) Li, M.; Zhang, Q.; Kurokawa, J.; Woo, J.; He, K.; Lu, Z.; Ohara, T.; Song, Y.; Streets, D. G.; Carmichael, G. R.; Cheng, Y.; Hong, C.; Huo, H.; Jiang, X.; Kang, S.; Liu, F.; Su, H.; Zheng, B. MIX: A Mosaic Asian Anthropogenic Emission Inventory under the International Collaboration Framework of the MICS-Asia and HTAP. Atmos. Chem. Phys. 2017, 17, 935-963.
- (31) Philip, S.; Martin, R. V.; Snider, G.; Weagle, C. L.; vanDonkelaar, A.; Brauer, M.; Henze, D. K.; Klimont, Z.; Venkataraman, C.; Guttikunda, S. K.; Zhang, Q. Anthropogenic fugitive, combustion, and industrial dust is significant, underrepresented fine particulate matter source in global atmospheric models. Environ. Res. Lett. 2017, 12 (044018), 044018.
- (32) Petters, M. D.; Kreidenweis, S. M. A Single Parameter Representation of Hygroscopic Growth and Cloud Condensation Nucleus Activity. Atmos. Chem. Phys. 2007, 7 (2), 1081-1091.
- (33) Wexler, A. S.; Clegg, S. L. Atmospheric Aerosol Models for Systems Including the Ions H⁺NH₄⁺Na⁺SO₄²⁻NO₃⁻Cl⁻Br⁻ and H₂O. J. Geophys. Res. 2002, 107 (D14), 4207.
- (34) Marais, E. A.; Jacob, D. J.; Jimenez, J. L.; Campuzano-Jost, P.; Day, D. A.; Hu, W.; Krechmer, J.; Zhu, L.; Kim, P. S.; Miller, C. C.; Fisher, J. A.; Travis, K.; Yu, K.; Hanisco, T. F.; Wolfe, G. M.; Arkinson, H. L.; Pye, H. O. T.; Froyd, K. D.; Liao, J.; McNeill, V. F. Aqueous-Phase Mechanism for Secondary Organic Aerosol Formation from Isoprene: Application to the Southeast United States and Co-Benefit of SO₂ Emission Controls. Atmos. Chem. Phys. **2016**, 16 (3), 1603–1618.
- (35) van Donkelaar, A.; Martin, R. V.; Brauer, M.; Kahn, R.; Levy, R.; Verduzco, C.; Villeneuve, P. J. Global Estimates of Ambient Fine Particulate Matter Concentrations from Satellite-Based Aerosol Optical Depth: Development and Application. Environ. Health Perspect. 2010, 118 (6), 847-855.
- (36) Li, C.; Martin, R. V.; vanDonkelaar, A.; Boys, B. L.; Hammer, M. S.; Xu, J. W.; Marais, E. A.; Reff, A.; Strum, M.; Ridley, D. A.; Crippa, M.; Brauer, M.; Zhang, Q. Trends in Chemical Composition of Global and Regional Population-Weighted Fine Particulate Matter Estimated for 25 Years. Environ. Sci. Technol. 2017, 51 (19), 11185-11195.
- (37) Lee, C. J.; Martin, R. V.; Henze, D. K.; Brauer, M.; Cohen, A.; van Donkelaar, A. Response of Global Particulate-Matter-Related Mortality

- to Changes in Local Precursor Emissions. Environ. Sci. Technol. 2015, 49 (7), 4335-4344.
- (38) Venkataraman, C.; Brauer, M.; Tibrewal, K.; Sadavarte, P.; Ma, Q.; Cohen, A.; Chaliyakunnel, S.; Frostad, J.; Klimont, Z.; Martin, R. V.; Millet, D. B.; Philip, S.; Walker, K.; Wa, S. Source Influence on Emission Pathways and Ambient PM_{2.5} Pollution over India (2015 - 2050). Atmos. Chem. Phys. 2018, 18, 8017-8039.
- (39) Lacey, F. G.; Henze, D. K.; Lee, C. J.; van Donkelaar, A.; Martin, R. V. Transient Climate and Ambient Health Impacts Due to National Solid Fuel Cookstove Emissions. Proc. Natl. Acad. Sci. U. S. A. 2017, 114 (6), 1269-1274.
- (40) Ma, Q.; Cai, S.; Wang, S.; Zhao, B.; Martin, R. V.; Brauer, M.; Cohen, A.; Jiang, J.; Zhou, W.; Hao, J.; Frostad, J.; Forouzanfar, M. H.; Burnett, R. T. Impacts of Coal Burning on Ambient PM25 Pollution in China. Atmos. Chem. Phys. Discuss. 2017, 17, 4477-4491.
- (41) Philip, S.; Martin, R. V.; van Donkelaar, A.; Lo, J. W.; Wang, Y.; Chen, D.; Zhang, L.; Kasibhatla, P. S.; Wang, S.; Zhang, Q.; Lu, Z.; Streets, D. G.; Bittman, S.; Macdonald, D. J. Global Chemical Composition of Ambient Fine Particulate Matter for Exposure Assessment. Environ. Sci. Technol. 2014, 48, 13060-13068.
- (42) Brauer, M.; Freedman, G.; Frostad, J.; vanDonkelaar, A.; Martin, R. V.; Dentener, F.; vanDingenen, R.; Estep, K.; Amini, H.; Apte, J. S.; Balakrishnan, K.; Barregard, L.; Broday, D.; Feigin, V.; Ghosh, S.; Hopke, P. K.; Knibbs, L. D.; Kokubo, Y.; Liu, Y.; Ma, S.; Morawska, L.; Sangrador, J. L. T.; Shaddick, G.; Anderson, H. R.; Vos, T.; Forouzanfar, M. H.; Burnett, R. T.; Cohen, A. Ambient Air Pollution Exposure Estimation for the Global Burden of Disease 2013. Environ. Sci. Technol. 2016, 50 (1), 79-88.
- (43) Krotkov, N. A.; McLinden, C. A.; Li, C.; Lamsal, L. N.; Celarier, E. A.; Marchenko, S. V.; Swartz, W. H.; Bucsela, E. J.; Joiner, J.; Duncan, B. N.; Boersma, K. F.; Veefkind, J. P.; Levelt, P. F.; Fioletov, V. E.; Dickerson, R. R.; Hao, H.; Lu, Z.; Streets, D. G. Aura OMI Observations of Regional SO 2 and NO 2 Pollution Changes from 2005 to 2015. Atmos. Chem. Phys. 2016, 16 (7), 4605-4629.
- (44) McLinden, C. A.; Fioletov, V.; Shephard, M. W.; Krotkov, N.; Li, C.; Martin, R. V.; Moran, M. D.; Joiner, J. Space-Based Detection of Missing Sulfur Dioxide Sources of Global Air Pollution. Nat. Geosci. **2016**, 9, 1-7.
- (45) Greenstone, M. The Impacts of Environmental Regulations on Industrial Activity: Evidence from the 1970 and 1977 Clean Air Act Amendments and the Census of Manufactures. J. Polit. Econ. 2001, 110 (6), 1175-1219,
- (46) Hand, J. L.; Schichtel, B. A.; Malm, W. C.; Pitchford, M. L. Particulate Sulfate Ion Concentration and SO 2 Emission Trends in the United States from the Early 1990s through 2010. Atmos. Chem. Phys. **2012**, *12*, 10353–10365.
- (47) Stjern, C. W.; Stohl, A.; Kristjánsson, J. E. Have Aerosols Affected Trends in Visibility and Precipitation in Europe? J. Geophys. Res. 2011, 116 (D2), 1–15.
- (48) Li, C.; Martin, R. V.; Boys, B. L.; van Donkelaar, A.; Ruzzante, S. Evaluation and Application of Multi-Decadal Visibility Data for Trend Analysis of Atmospheric Haze. Atmos. Chem. Phys. 2016, 16, 2435-
- (49) Clarisse, L.; Clerbaux, C.; Dentener, F.; Hurtmans, D.; Coheur, P.-F. Global Ammonia Distribution Derived from Infrared Satellite Observations. Nat. Geosci. 2009, 2 (7), 479-483.
- (50) Kharol, S. K.; Martin, R. V.; Philip, S.; Vogel, S.; Henze, D. K.; Chen, D.; Wang, Y.; Zhang, Q.; Heald, C. L. Persistent Sensitivity of Asian Aerosol to Emissions of Nitrogen Oxides. Geophys. Res. Lett. 2013, 40, 1021-1026.
- (51) Xu, R. T.; Pan, S. F.; Chen, J.; Chen, G. S.; Yang, J.; Dangal, S. R. S.; Shepard, J. P.; Tian, H. Q. Half-Century Ammonia Emissions From Agricultural Systems in Southern Asia: Magnitude, Spatiotemporal Patterns, and Implications for Human Health. GeoHealth 2018, 2, 40-
- (52) Kim, P. S.; Jacob, D. J.; Fisher, J. A.; Travis, K.; Yu, K.; Zhu, L.; Yantosca, R. M.; Sulprizio, M. P.; et al. Sources, Seasonality, and Trends of Southeast US Aerosol: An Integrated Analysis of Surface, Aircraft,

- and Satellite Observations with the GEOS-Chem Chemical Transport Model. *Atmos. Chem. Phys.* **2015**, *15*, 10411–10433.
- (53) Silvern, R. F.; Jacob, D. J.; Kim, P. S.; Marais, E. A.; Turner, J. R.; Campuzano-Jost, P.; Jimenez, J. L. Inconsistency of Ammonium—Sulfate Aerosol Ratios with Thermodynamic Models in the Eastern US: A Possible Role of Organic Aerosol. *Atmos. Chem. Phys.* **2017**, *17* (8), 5107—5118.
- (54) Paulot, F.; Jacob, D. J.; Pinder, R. W.; Bash, J. O.; Travis, K.; Henze, D. K. Ammonia Emissions in the United States, European Union, and China Derived by High-Resolution Inversion of Ammonium Wet Deposition Data: Interpretation with a New Agricultural Emissions Inventory (MASAGE NH₃). J. Geophys. Res. Atmos. 2014, 119, 4343–4364.
- (55) Lu, Z.; Zhang, Q.; Streets, D. G. Sulfur Dioxide and Primary Carbonaceous Aerosol Emissions in China and India, 1996 2010. *Atmos. Chem. Phys.* **2011**, *11*, 9839–9864.
- (56) Bonjour, S.; Adair-Rohani, H.; Wolf, J.; Bruce, N. G.; Mehta, S.; Prüss-Ustün, A.; Lahiff, M.; Rehfuess, E. A.; Mishra, V.; Smith, K. R. Solid Fuel Use for Household Cooking: Country and Regional Estimates for 1980 2010. *Environ. Health Perspect.* **2013**, *121* (7), 784–791.
- (57) Zhang, L.; Liu, L.; Zhao, Y.; Gong, S.; Zhang, X.; Henze, D. K.; Capps, S. L.; Fu, T.-M.; Zhang, Q.; Wang, Y. Source Attribution of Particulate Matter Pollution over North China with the Adjoint Method. *Environ. Res. Lett.* **2015**, *10*, 084011.
- (58) Klimont, Z.; Smith, S. J.; Cofala, J. The Last Decade of Global Anthropogenic Sulfur Dioxide: 2000–2011 Emissions. *Environ. Res. Lett.* 2013, 8 (1), 014003.
- (59) Xu, Y. Improvements in the Operation of SO2 Scrubbers in Chinas Coal Power Plants. *Environ. Sci. Technol.* **2011**, 45 (2), 380–385.
- (60) Pinder, R. W.; Adams, P. J. Ammonia Emission Controls as a Cost-Effective Strategy for Reducing Atmospheric Particulate Matter in the Eastern United States. *Environ. Sci. Technol.* **2007**, *41* (2), 380–386.
- (61) Wang, Y.; Zhang, Q. Q.; He, K.; Zhang, Q.; Chai, L. Sulfate-Nitrate-Ammonium Aerosols over China: Response to 2000 2015 Emission Changes of Sulfur Dioxide, Nitrogen Oxides, and Ammonia. *Atmos. Chem. Phys.* **2013**, *13*, 2635–2652.
- (62) Heald, C. L.; Collett, J.; Lee, T.; Benedict, K. B.; Schwandner, F. M.; Li, Y.; Clarisse, L.; Hurtmans, D. R.; VanDamme, M.; Clerbaux, C.; Coheur, P. F.; Philip, S.; Martin, R.; Pye, H. Atmospheric Ammonia and Particulate Inorganic Nitrogen over the United States. *Atmos. Chem. Phys.* **2012**, *12* (21), 10295–10312.
- (63) Ram, K.; Sarin, M. M.; Tripathi, S. N. Temporal Trends in Atmospheric PM_{2.5}, PM₁₀, Elemental Carbon, Organic Carbon, Water-Soluble Organic Carbon, and Optical Properties: Impact of Biomass Burning Emissions in the Indo-Gangetic Plain. *Environ. Sci. Technol.* **2012**, 46 (2), 686–695.
- (64) Tare, V.; Tripathi, S. N.; Chinnam, N.; Srivastava, A. K.; Dey, S.; Manar, M.; Kanawade, V. P.; Agarwal, A.; Kishore, S.; Lal, R. B.; Sharma, M. Measurements of Atmospheric Parameters during Indian Space Research Organization Geosphere Biosphere Programme Land Campaign II at a Typical Location in the Ganga Basin: 1. Physical and Optical Properties. *J. Geophys. Res. Atmos.* 2006, 111 (23), 7278.
- (65) Kumar, M.; Raju, M. P.; Singh, R. K.; Singh, A. K.; Singh, R. S.; Banerjee, T. Wintertime Characteristics of Aerosols over Middle Indo-Gangetic Plain: Vertical Profile, Transport and Radiative Forcing. *Atmos. Res.* **2017**, *183*, 268–282.
- (66) Satish, R.; Shamjad, P.; Thamban, N.; Tripathi, S.; Rastogi, N. Temporal Characteristics of Brown Carbon over the Central Indo-Gangetic Plain. *Environ. Sci. Technol.* **2017**, *S1* (12), 6765–6772.
- (67) Shamjad, P. M.; Tripathi, S. N.; Pathak, R.; Hallquist, M.; Arola, A.; Bergin, M. H. Contribution of Brown Carbon to Direct Radiative Forcing over the Indo-Gangetic Plain. *Environ. Sci. Technol.* **2015**, 49 (17), 10474–10481.
- (68) Begum, B. A.; Hossain, A.; Nahar, N.; Markwitz, A.; Hopke, P. K. Organic and Black Carbon in PM_{2.5} at an Urban Site at Dhaka, Bangladesh. *Aerosol Air Qual. Res.* **2012**, *12* (6), 1062–1072.

- (69) Lu, Z.; Streets, D. G.; de Foy, B.; Krotkov, N. A. Ozone Monitoring Instrument Observations of Interannual Increases in SO_2 Emissions from Indian Coal-Fired Power Plants during 2005 2012. *Environ. Sci. Technol.* **2013**, 47, 13993-14000.
- (70) Fioletov, V. E.; McLinden, C. A.; Krotkov, N.; Li, C.; Joiner, J.; Theys, N.; Carn, S.; Moran, M. D. A Global Catalogue of Large SO_2 Sources and Emissions Derived from the Ozone Monitoring Instrument. *Atmos. Chem. Phys. Discuss.* **2016**, No. May, 1–45.
- (71) Chinnam, N.; Dey, S.; Tripathi, S. N.; Sharma, M. Dust Events in Kanpur, Northern India: Chemical Evidence for Source and Implications to Radiative Forcing. *Geophys. Res. Lett.* **2006**, 33 (8), 1–4.
- (72) Gautam, R.; Liu, Z.; Singh, R. P.; Hsu, N. C. Two Contrasting Dust-Dominant Periods over India Observed from MODIS and CALIPSO Data. *Geophys. Res. Lett.* **2009**, *36* (6), 1–5.
- (73) Zheng, Y.; Zhao, T.; Che, H.; Liu, Y.; Han, Y.; Liu, C.; Xiong, J.; Liu, J.; Zhou, Y. A 20-Year Simulated Climatology of Global Dust Aerosol Deposition. *Sci. Total Environ.* **2016**, *557*–*558*, 861–868.
- (74) Dey, S.; Tripathi, S. N.; Singh, R. P.; Holben, B. N. Influence of Dust Storms on the Aerosol Optical Properties over the Indo-Gangetic Basin. *J. Geophys. Res.* **2004**, *109* (20), 1–13.
- (75) Begum, B. A.; Kim, E.; Biswas, S. K.; Hopke, P. K. Investigation of Sources of Atmospheric Aerosol at Urban and Semi-Urban Areas in Bangladesh. *Atmos. Environ.* **2004**, *38* (19), 3025–3038.
- (76) Misra, A.; Gaur, A.; Bhattu, D.; Ghosh, S.; Dwivedi, A. K.; Dalai, R.; Paul, D.; Gupta, T.; Tare, V.; Mishra, S. K.; Singh, S.; Tripathi, S. N. An Overview of the Physico-Chemical Characteristics of Dust at Kanpur in the Central Indo-Gangetic Basin. *Atmos. Environ.* **2014**, 97, 386–396.
- (77) Koplitz, S. N.; Mickley, L. J.; Marlier, M. E.; Buonocore, J. J.; Kim, P. S.; Liu, T.; Sulprizio, M. P.; DeFries, R. S.; Jacob, D. J.; Schwartz, J.; Pongsiri, M.; Myers, S. S. Public Health Impacts of the Severe Haze in Equatorial Asia in September—October 2015: Demonstration of a New Framework for Informing Fire Management Strategies to Reduce Downwind Smoke Exposure. *Environ. Res. Lett.* **2016**, *11* (9), 94023.
- (78) Chang, C.-H.; Hsiao, Y.-L.; Hwang, C. Evaluating Spatial and Temporal Variations of Aerosol Optical Depth and Biomass Burning over Southeast Asia Based on Satellite Data Products. *Aerosol Air Qual. Res.* **2015**, *15* (7), 2625–2640.
- (79) Lee, H. H.; Bar-Or, R. Z.; Wang, C. Biomass Burning Aerosols and the Low-Visibility Events in Southeast Asia. *Atmos. Chem. Phys.* **2017**, *17* (2), 965–980.
- (80) Boucher, O.; Moulin, C.; Belviso, S.; Aumont, O.; Bopp, L.; Cosme, E.; vonKuhlmann, R.; Lawrence, M. G.; Pham, M.; Reddy, M. S.; Sciare, J.; Venkataraman, C. Sensitivity Study of Dimethylsulphide (DMS) Atmospheric Concentrations and Sulphate Aerosol Indirect Radiative Forcing to the DMS Source Representation and Oxidation. *Atmos. Chem. Phys. Discuss.* **2002**, 2 (4), 1181–1216.
- (81) Lestari, P.; Mauliadi, Y. D. Source Apportionment of Particulate Matter at Urban Mixed Site in Indonesia Using PMF. *Atmos. Environ.* **2009**, 43 (10), 1760–1770.
- (82) Ridley, D. A.; Heald, C. L.; Ford, B. North African Dust Export and Deposition: A Satellite and Model Perspective. *J. Geophys. Res. Atmos.* **2012**, *117* (2), 1–21.
- (83) Generoso, S.; Bréon, F.-M.; Balkanski, Y.; Boucher, O.; Schulz, M. Improving the Seasonal Cycle and Interannual Variations of Biomass Burning Aerosol Sources. *Atmos. Chem. Phys.* **2003**, 3 (4), 1211–1222.
- (84) Latham, J.; Cumani, R.; Rosati, I.; Bloise, M. FAO Global Land Cover SHARE; Food and Agriculture Organization of the United Nations: 2014.
- (85) Reddington, C. L.; Butt, E. W.; Ridley, D. A.; Artaxo, P.; Morgan, W. T.; Coe, H.; Spracklen, D. V. Air Quality and Human Health Improvements from Reductions in Deforestation-Related Fire in Brazil. *Nat. Geosci.* **2015**, *8*, 768–771.
- (86) Freitas, S. R.; Longo, K. M.; SilvaDias, M. A. F.; SilvaDias, P. L.; Chatfield, R.; Prins, E.; Artaxo, P.; Grell, G. A.; Recuero, F. S. Monitoring the Transport of Biomass Burning Emissions in South America. *Environ. Fluid Mech.* **2005**, 5 (1–2), 135–167.

- (87) Graham, B.; Falkovich, A. H.; Rudich, Y.; Maenhaut, W.; Guyon, P.; Andreae, M. O. Local and Regional Contributions to the Atmospheric Aerosol over Tel Aviv, Israel: A Case Study Using Elemental, Ionic and Organic Tracers. *Atmos. Environ.* **2004**, *38*, 1593–1604
- (88) Formenti, P.; Andreae, M. O.; Andreae, T. W.; Galani, E.; Vasaras, A.; Zerefos, C.; Amiridis, V.; Orlovsky, L.; Karnieli, A.; Wendisch, M.; Wex, H.; Holben, B. N.; Maenhaut, W.; Lelieveld, J. Aerosol Optical Properties and Large-Scale Transport of Air Masses: Mediterranean during Summer 1998. *J. Geophys. Res.* **2001**, *106*, 9807–9826.
- (89) Balakrishnan, K.; Ghosh, S.; Ganguli, B.; Sambandam, S.; Bruce, N.; Barnes, D. F.; Smith, K. R. State and National Household Concentrations of PM_{2.5} from Solid Cookfuel Use: Results from Measurements and Modeling in India for Estimation of the Global Burden of Disease. *Environ. Health* **2013**, *12*, 77.
- (90) Anenberg, S. C.; Horowitz, L. W.; Tong, D. Q.; West, J. J. An Estimate of the Global Burden of Anthropogenic Ozone and Fine Particulate Matter on Premature Human Mortality Using Atmospheric Modeling. *Environ. Health Perspect.* **2010**, *118* (9), 1189–1195.
- (91) Lin, J.; Pan, D.; Davis, S. J.; Zhang, Q.; He, K.; Wang, C.; Streets, D. G.; Wuebbles, D. J.; Guan, D. China's International Trade and Air Pollution in the United States. *Proc. Natl. Acad. Sci. U. S. A.* **2014**, *111*, 1736–1741.
- (92) Zhang, Q.; Jiang, X.; Tong, D.; Davis, S. J.; Zhao, H.; Geng, G.; et al. Transboundary Health Impacts of Transported Global Air Pollution and International Trade. *Nature* **2017**, *543* (7647), 705–709.
- (93) Prospero, J. M.; Ginoux, P.; Torres, O.; Nicholson, S. E.; Gill, T. E. Environmental Characterization of Global Sources of Atmospheric Soil Dust Identified with the NIMBUS 7 Total Ozone Mapping Spectrometer (TOMS) Absorbing Aerosol Product. *Rev. Geophys.* **2002**, *40*, 1002.
- (94) Ginoux, P.; Chin, M.; Tegen, I.; Prospero, J. M.; Holben, B.; Dubovik, O.; Lin, S.-J. Sources and Distributions of Dust Aerosols Simulated with the GOCART Model. *J. Geophys. Res.* **2001**, *106*, 20255–20273.
- (95) Conibear, L.; Butt, E. W.; Knote, C.; Arnold, S. R.; Spracklen, D. V. Residential Energy Use Emissions Dominate Health Impacts from Exposure to Ambient Particulate Matter in India. *Nat. Commun.* **2018**, 9 (1), 1–9.
- (96) Silva, R. A.; Adelman, Z.; Fry, M. M.; West, J. J. The Impact of Individual Anthropogenic Emissions Sectors on the Global Burden of Human Mortality Due to Ambient Air Pollution. *Environ. Health Perspect.* **2016**, 124 (11), 1776–1784.
- (97) Zhang, L.; Kok, J. F.; Henze, D. K.; Li, Q.; Zhao, C. Improving Simulations of Fine Dust Surface Concentrations over the Western United States by Optimizing the Particle Size Distribution. *Geophys. Res. Lett.* **2013**, *40* (12), 3270–3275.
- (98) Ridley, D. A.; Heald, C. L.; Kok, J. F.; Zhao, C. An Observationally-Constrained Estimate of Global Dust Aerosol Optical Depth. *Atmos. Chem. Phys. Discuss.* **2016**, No. May, 1–31.